The facile synthesis of graphene nanoplatelet–lead styphnate composites and their depressed electrostatic hazards

ARTICLE · OCTOBER 2013

DOI: 10.1039/C3TA13177G

6 AUTHORS, INCLUDING:

Zhimin Li
The Hong Kong University of Science and T…
39 PUBLICATIONS **167** CITATIONS
SEE PROFILE

Tong-Lai Zhang
Beijing Institute of Technology
273 PUBLICATIONS **1,136** CITATIONS
SEE PROFILE

Jian-Guo Zhang
Beijing Institute of Technology
312 PUBLICATIONS **1,579** CITATIONS
SEE PROFILE

Li Yang
Nanjing Medical University
155 PUBLICATIONS **1,621** CITATIONS
SEE PROFILE

Journal of Materials Chemistry A

RSC Publishing

COMMUNICATION

View Article Online
View Journal | View Issue

Cite this: *J. Mater. Chem. A*, 2013, **1**, 12710

Received 12th August 2013
Accepted 27th August 2013

DOI: 10.1039/c3ta13177g

www.rsc.org/MaterialsA

The facile synthesis of graphene nanoplatelet–lead styphnate composites and their depressed electrostatic hazards†

Zhi-Min Li, Ming-Rui Zhou, Tong-Lai Zhang,* Jian-Guo Zhang, Li Yang and Zun-Ning Zhou

Graphene nanoplatelet–lead styphnate composites (GLS) were prepared either by adding graphene nanoplatelets (GNP) to the reaction solution or by coating normal lead styphnate (LS) with GNP. The composites exhibited excellent anti-electrostatic performance with depressed electrostatic spark sensitivity and static electricity accumulation.

The sensitive explosives used to initiate devices like primers and detonators are called primary explosives. Detonation of the primary explosive initiates the secondary booster or main-charge explosive/propellant.[1,2] Lead styphnate (LS, also known as lead trinitroresorcinate) was first identified in 1907 and is one of the most widely used primary explosives in both military and civilian fields, due to its excellent properties, especially its sensitivity to flame.[3–7] However, LS is highly non-conductive *i.e.*, it can easily accumulate electrostatic charges after coming into contact with and separating from other objects. Once the electric potential exceeds the breakdown voltage of the surrounding atmosphere, an electrostatic discharge (ESD) occurs, and even a low energy spark of the order of 0.2–0.3 mJ is enough to ignite LS.[8,9] Many terrible accidents involving explosives have been caused by ESD.[10–14] Therefore, research into antistatic modification is meaningful, in order to reduce risks in the processing and handling of LS.

Since the independent existence of graphene was reported by Geim and coworkers,[15,16] it has been considered to be a promising candidate in many applications due to its extraordinary mechanical, electric, thermal and optical properties.[17–23] Graphene nanoplatelets (GNPs) *i.e.*, multilayer graphene has attracted considerable attention in the areas of composites,[24–31] solar cells[32] and electrocatalysts.[33] Recently, experimental[34–36] and theoretical[37,38] studies on the application of graphene for energetic materials have become an interesting issue. Graphene/metal nanoparticle[39,40] and ionic liquid/graphene composites[41,42] as well as nitrogen-doped graphene[43] have been used for 2,4,6-trinitrotoluene (TNT) detection. In view of its preeminent thermal and electrical conductivity, GNP was selected to improve the anti-electrostatic properties of LS in this study.

The starting materials used in the present investigation for the preparation of LS were purchased from commercial suppliers and used without further purification unless otherwise noted. LS was obtained by the dropwise addition of a magnesium styphnate solution to a solution of lead nitrate at a temperature of 70–75 °C, where magnesium styphnate was first prepared from the reaction of styphnic acid and magnesium oxide. GNP (purity: >99.5 wt%, layers: <30, thickness: 4–20 nm, diameter: 5–10 μm) was purchased from Chengdu Organic Chemicals Co. Ltd. CAS, (China). Two methods were applied to prepare the GNP–LS composites *via* the addition of GNP: one was dispersing GNP into the reaction solution of lead nitrate, and the other was coating the normal LS with GNP using an adhesive. A schematic diagram illustrating the preparation of GLS is shown in Fig. 1. Details for the preparation of GLS(I) and GLS(II) can be found in section S1.†

The granular appearance of the normal LS, GLS(I) and GLS(II) is shown in Fig. 2a. GNP and the crystals of LS were uniformly composited together, while the color of GLS changed to gray or black. The size of the particles of GLS(II) is bigger than that of GLS(I) due to the crystals being bonded by an adhesive. Raman spectroscopy was used to study the surface structure of the composites. Fig. 2b shows the Raman spectra of GNP, normal LS and GLS. The Raman shifts featured in both GNP and LS were found in the spectrum of the obtained GLS composites. In order to further confirm the relationship between the two individual units, X-ray diffraction (XRD) patterns (Fig. 2c) of the above samples were obtained. The XRD pattern of GLS reveals that the characteristic sharp peak of GNP located at $2\theta \approx 26^\circ$ does not appear, confirming that GNP is

State Key Laboratory of Explosion Science and Technology, Beijing Institute of Technology, Beijing 100081, P. R. China. E-mail: ztlbit@bit.edu.cn; Fax: +86-10-68911202; Tel: +86-10-68911202

† Electronic supplementary information (ESI) available. See DOI: 10.1039/c3ta13177g

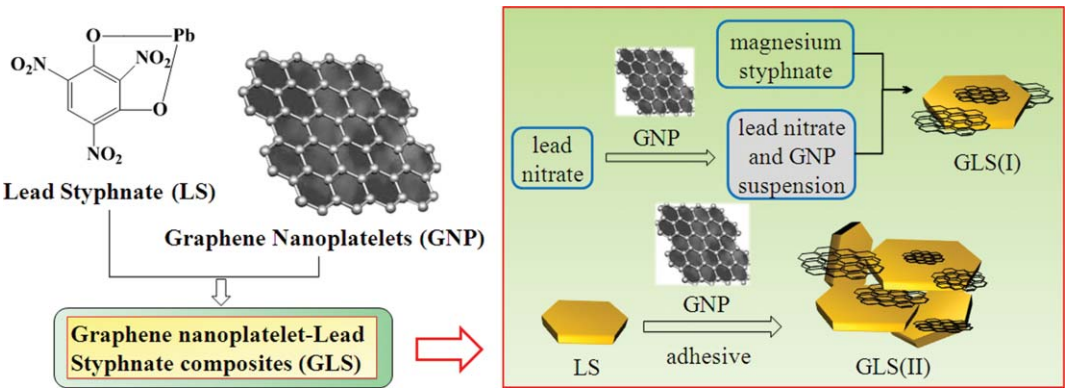

Fig. 1 Schematic representation of the preparation of GLS.

well composited with LS. Similar results were also found in a previous report.[44]

A field-emission scanning electron microscope (FE-SEM) equipped with an energy dispersive spectrometer was employed to characterize the morphology and composition of the products. Fig. 3a and inset a1 show SEM images of the normal LS crystals and GNP, respectively. An SEM image of GLS is shown in Fig. 3b, in which it is clearly shown that GNP is coated on to some places of the LS crystals. Energy dispersive spectroscopy (EDS) analysis on the GNP coated part of LS (Fig. 3c, area 1) reveals that the sample is mainly composed of the elements C and Pb, with the higher C content being ascribed to the presence of GNP. In contrast, a much higher content of Pb was obtained when the part of LS without the GNP covering (area 2) was examined. To further demonstrate the "GNP covered LS" structure, elemental mapping technology was used, and the results (Fig. 3d and e) show an obvious C profile distributed along the graphene nanoplatelets.

The conductivity of GLS was noticeably improved, due to the extraordinary electroconductivity of GNP. The surface resistivity of LS is 3.5×10^{15} Ω, whereas GLS(I) (1 wt% GNP) and GLS(II) (1 wt% GNP) have reduced values of 5.8×10^{10} Ω and 2.2×10^{12} Ω, respectively. The volume resistivity of LS, GLS(I) (1 wt% GNP) and GLS(II) (1 wt% GNP) are 1.9×10^{16} Ω cm, 3.1×10^{11} Ω cm and 7.6×10^{13} Ω cm, respectively. The difference in the conductivity between GLS(I) and GLS(II) is caused by the different size of the particles, which results in a variation of the interspacing between them.

In order to characterize the dangerous reactions of GLS towards stimulus from electrostatic discharge, the electrostatic spark sensitivity was tested. Values of E_{50} for GLS with different

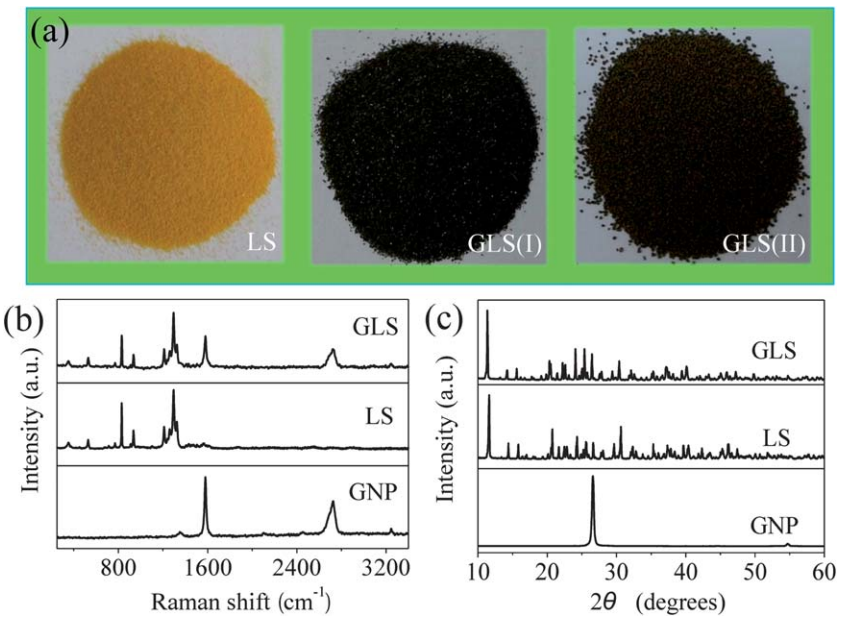

Fig. 2 (a) Granular appearances of normal LS and the GLS composites, as well as the (b) Raman spectra and (c) XRD patterns of GNP, normal LS and GLS.

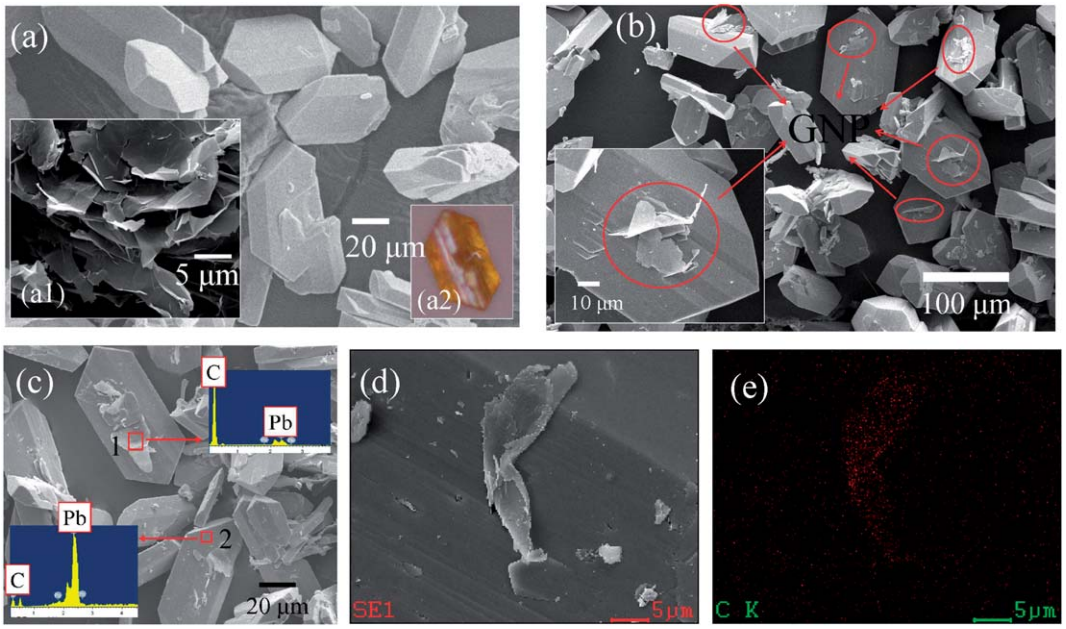

Fig. 3 SEM images of (a) normal LS, (a1) the raw GNP material and (a2) the crystal morphology of LS. (b) An SEM image of GLS. (c) EDS spectrum of GLS. (d) An SEM image of a GNP covered LS crystal and (e) the corresponding elemental mapping image for carbon.

GNP content are shown in Fig. 4a. The E_{50} of normal LS is 0.14 mJ. We clearly observe that the E_{50} of GLS(I) does not change very much when the content of GNP is less than 1 wt%. Whereas, the E_{50} of GLS(II) increases with increasing GNP content, when it is below 1 wt%. When the GNP content is more than 1 wt%, the E_{50} of GLS basically stabilizes and no longer decreases much, with values of about 0.4 mJ and 0.5 mJ for GLS(I) and GLS(II), respectively. A GNP content of 1 wt% is the best choice to prepare GNP–LS composites. The adhesive bonding the LS crystals together and the coating of GNP makes it harder to ignite GLS (II) using an electrostatic spark.

It is well known that electrostatic charges may be generated when two particles of different materials come into contact and then separate. This is called "triboelectric charging". For explosives, static electricity accumulation is used to characterize the electrostatic charge generated from friction with other objects. Different flumes are used to simulate the tribo-electrification between an explosive and the various materials of devices used during the processes of preparation and application. In this work, the following flumes were selected: stainless steel, aluminium, fabroil, conductive rubber and shellac painted kraft. The static electricity accumulation of GLS with various GNP content are displayed in Fig. 4b and c. The results show that the static electricity accumulation of GLS is reduced a lot compared to normal LS using each of the five flumes. The static electricity accumulation values of normal LS are −18.29, −13.48, −11.94, −10.36 and −9.69 nC g^{-1}, tested using the shellac painted kraft, aluminium, fabroil, conductive rubber and stainless steel flumes, respectively. Fig. 4(b) shows the static electricity accumulation of GLS(I), which decreased with increasing GNP content. The static electricity accumulation values of GLS(I) with 1 wt% GNP were reduced to −4.95, −2.93, −2.59, −2.6 and −2.52 nC g^{-1} for the shellac painted kraft, aluminium, fabroil, conductive rubber and stainless steel flumes, respectively. Fig. 4(c) shows the static electricity accumulation of GLS(II) with various GNP contents. As the content of GNP increased, the static electricity accumulation of GLS(II) heavily decreased. When the GNP content is higher than 0.5 wt %, the electrostatic charges are almost eliminated. The decrease in the static electricity accumulation of GLS can be attributed to the presence of GNP and its excellent conductivity. For GLS(II), the crystals of LS are bonded together to form big granules, which also decreases static electricity accumulation. In conclusion, the addition of GNP to LS can greatly improve the anti-electrostatic performance. The best GNP content for applications was identified to be 1 wt%.

In order to assess the thermal performance of GLS (1 wt% GNP), differential scanning calorimetry was carried out at a heating rate of 10 °C min^{-1}. The 5 s delay explosion temperatures, flame sensitivity, impact sensitivity and friction sensitivity were tested in order to comprehensively characterize the safety of GLS. All of the sensitivity data for GLS were compared with normal LS and are listed in Table 1. The thermal and flame sensitivity of GLS has not varied much. GLS is less sensitive to mechanical stimuli such as friction and impact. Generally, the obtained GNP–LS composites are safer than normal LS, when used as primary explosives.

In summary, in this work graphene nanoplatelet–lead styphnate composites were synthesized for the first time, using a facile method. The obtained GLS composites exhibited excellent anti-electrostatic performances with depressed electrostatic hazards. With 1 wt% GNP, the GLS composites may be applied in many igniters as a new electrostatically safe primary explosive.

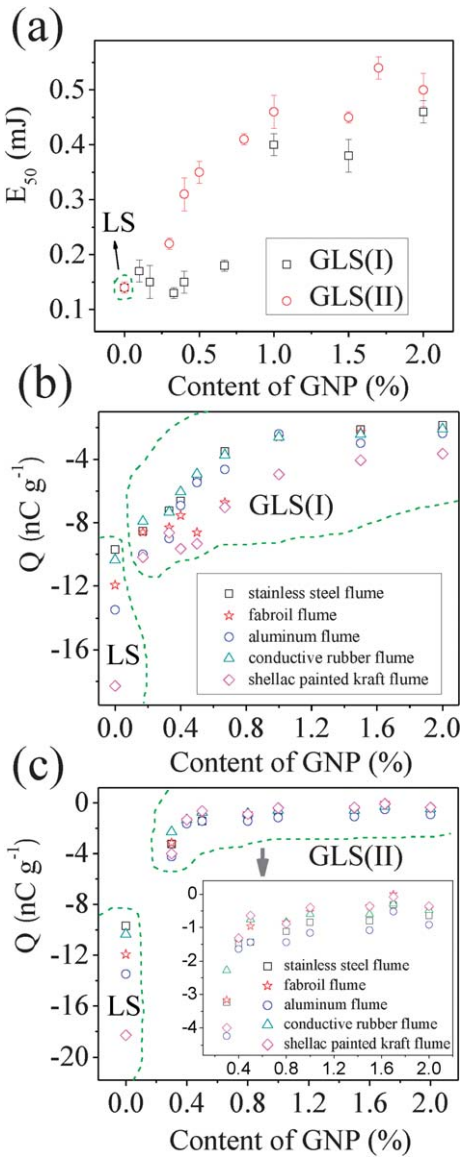

Fig. 4 (a) The electrostatic spark sensitivity and (b and c) static electricity accumulation of GLS composites with various content of GNP.

Table 1 The sensitivities of GLS compared with normal LS[a]

Sample	T_p/°C	T_5/°C	$H_{50}(F)$/cm	P/%	$H_{50}(I)$/cm
Normal LS	300.2	323	47	68	12.1
GLS(I)	300.5	324	49	48	17.7
GLS(II)	296.6	321	42	52	16.5

[a] T_p: peak temperature of thermal decomposition determined using DSC; T_5: 5 s delay explosion temperature; $H_{50}(F)$: 50% firing height for flame; P: Probability of fire from friction; $H_{50}(I)$: 50% firing height for impact.

Acknowledgements

This work was financially supported by National Basic Research Program of China and the Doctoral Candidate Innovation Research Support Program by Science & Technology Review (kjdb201001-2). We gratefully acknowledge Prof. Bo Wang, Prof. Liang-Ti Qu and Dr Chuan-Gang Hu (School of Chemistry, Beijing Institute of Technology) for their kind assistance for the revision of this paper.

References

1 M. H. V. Huynh, M. D. Coburn, T. J. Meyer and M. Wetzler, *Proc. Natl. Acad. Sci. U. S. A.*, 2006, **103**, 10322.
2 M. H. V. Huynh, M. A. Hiskey, T. J. Meyer and M. Wetzler, *Proc. Natl. Acad. Sci. U. S. A.*, 2006, **103**, 5409.
3 N. Orbovic and C. L. Codoceo, *Propellants, Explos., Pyrotech.*, 2008, **33**, 459.
4 T. E. Larson, P. Dimas and C. E. Hannaford, *Inst. Phys. Conf. Ser.*, 1991, **118**, 107.
5 V. N. Borzdun, N. N. Dvorovenko and S. M. Ryabykh, *High Energy Chem.*, 2002, **36**, 438.
6 H. Y. Feng, L. Zhang, S. G. Zhu, Y. Li and R. Q. Shen, *Heat Mass Transfer*, 2011, **48**, 585.
7 W. H. Zhu and H. M. Xiao, *J. Phys. Chem. B*, 2009, **113**, 10315.
8 M. B. Talawar, A. P. Agrawal, M. Anniyappan, D. S. Wani, M. K. Bansode and G. M. Gore, *J. Hazard. Mater.*, 2006, **137**, 1074.
9 G. X. Li and C. Y. Wang, *J. Electrost.*, 1982, **11**, 319.
10 S. Darin, O. Douglas and B. B. Andrew, *Propellants, Explos., Pyrotech.*, 1998, **23**, 34.
11 Z. M. Li, T. L. Zhang, L. Yang, Z. N. Zhou and J. G. Zhang, *Sci Tech Rev*, 2011, **29**, 73.
12 M. Roux, M. Auzanneau and C. Brassy, *Propellants, Explos., Pyrotech.*, 1993, **18**, 317.
13 M. Auzanneau and M. Roux, *Propellants, Explos., Pyrotech.*, 1995, **20**, 96.
14 M. Lu and Y. B. Zhao, *Acta Armamentarii*, 2009, **30**, 1602.
15 J. C. Meyer, A. K. Geim, M. I. Katsnelson, K. S. Novoselov, T. J. Booth and S. Roth, *Nature*, 2007, **446**, 60.
16 K. S. Novoselov, A. K. Geim, S. V. Morozov, D. Jiang, Y. Zhang, S. V. Dubonos, I. V. Grigorieva and A. A. Firsov, *Science*, 2004, **306**, 666.
17 S. Sattayasamitsathit, Y. Gu, K. Kaufmann, W. Jia, X. Xiao, M. Rodriguez, S. Minteer, J. Cha, D. B. Burckel, C. Wang, R. Polsky and J. Wang, *J. Mater. Chem. A*, 2013, **1**, 1639.
18 S. Wangmo, R. Song, L. Wang, W. Jin, D. Ding, Z. Wang and R. Q. Zhang, *J. Mater. Chem.*, 2012, **22**, 23380.
19 P. Han, W. Ma, S. Pang, Q. Kong, J. Yao, C. Bi and G. Cui, *J. Mater. Chem. A*, 2013, **1**, 5949.
20 Y. Ye and L. Dai, *J. Mater. Chem.*, 2012, **22**, 24224.
21 X. Xiao, J. R. Michael, T. Beechem, A. McDonald, M. Rodriguez, M. T. Brtunbach, T. N. Lambert, C. M. Washburn, J. Wang, S. M. Brozik, D. R. Wheeler, D. B. Burckel and R. Polsky, *J. Mater. Chem.*, 2012, **22**, 23749.
22 T. Stergiopoulos, M. Bidikoudi, V. Likodimos and P. Falaras, *J. Mater. Chem.*, 2012, **22**, 24430.
23 M. He, J. Jung, F. Qiu and Z. Lin, *J. Mater. Chem.*, 2012, **22**, 24254.
24 X. L. Yang, Z. C. Wang, M. Z. Xu, R. Zhao and X. B. Liu, *Mater. Des.*, 2013, **44**, 74.

25 R. G. Mendes, A. Bachmatiuk, A. A. El-Gendy, S. Melkhanova, R. Klingeler, B. Büchner and M. H. Rümmeli, *J. Phys. Chem. C*, 2012, **116**, 23749.
26 K. M. F. Shahil and A. A. Balandin, *Nano Lett.*, 2012, **12**, 861.
27 J. F. Wang, H. Q. Xie and Z. Xin, *J. Nanopart. Res.*, 2012, **14**, 952.
28 W. L. Song, W. Wang, L. M. Veca, C. Y. Kong, M. S. Cao, P. Wang, M. J. Meziani, H. J. Qian, G. E. LeCroy, L. Cao and Y. P. Sun, *J. Mater. Chem.*, 2012, **22**, 17133.
29 B. Li, E. Olson, A. Perugini and W. H. Zhong, *Polymer*, 2011, **52**, 5606.
30 K. Chu, W. S. Li, C. C. Jia and F. L. Tang, *Appl. Phys. Lett.*, 2012, **101**, 211903.
31 K. M. F. Shahil and A. A. Balandin, *Solid State Commun.*, 2012, **152**, 1331.
32 L. Kavan, J. H. Yum, M. K. Nazeeruddin and M. Grätzel, *ACS Nano*, 2011, **5**, 9171.
33 Y. Choi, M. Gu, J. Park, H. K. Song and B. S. Kim, *Adv. Energy Mater.*, 2012, **2**, 1510.
34 K. Kappagantula, M. L. Pantoya and E. M. Hunt, *J. Appl. Phys.*, 2012, **112**, 024902.
35 D. Krishnan, F. Kim, J. Luo, R. Cruz-Silva, L. J. Cote, H. D. Jang and J. Huang, *Nano Today*, 2012, **7**, 137.
36 Y. Shi and L. Li, *J. Mater. Chem.*, 2011, **21**, 3277.
37 C. Y. Zhang, X. Cao and B. Xiang, *J. Phys. Chem. C*, 2010, **114**, 22684.
38 M. Smeu, F. Zahid, W. Ji, H. Guo, M. Jaidann and H. Abou-Rachid, *J. Phys. Chem. C*, 2011, **115**, 10985.
39 M. Liu and W. Chen, *Biosens. Bioelectron.*, 2013, **46**, 68.
40 Y. Yu, Q. Cao, M. Zhou and H. Cui, *Biosens. Bioelectron.*, 2013, **43**, 137.
41 S. Guo, D. Wen, Y. Zhai, S. Dong and E. Wang, *Biosens. Bioelectron.*, 2011, **26**, 3475.
42 C. X. Guo, Z. S. Lu, Y. Lei and C. M. Li, *Electrochem. Commun.*, 2010, **12**, 1237.
43 T. W. Chen, J. Y. Xu, Z. H. Sheng, K. Wang, F. B. Wang, T. M. Liang and X. H. Xia, *Electrochem. Commun.*, 2012, **16**, 30.
44 Z. Tang, X. Chen, H. Chen, L. Wu and X. Yu, *Angew. Chem., Int. Ed.*, 2013, **52**, 5832.

